# Direct Formation of Thin Single Crystals of Organic Semiconductors onto a Substrate

Takeshi Yamao,* Tomoharu Miki, Hiroshi Akagami, Yoshihiro Nishimoto, Satoshi Ota,† and Shu Hotta

*Department of Macromolecular Science and Engineering, Kyoto Institute of Technology, Matsugasaki, Sakyo-ku, Kyoto 606-8585, Japan*

*Received April 18, 2007. Revised Manuscript Received May 24, 2007*

We have developed a novel and convenient method of crystal growth in a liquid phase. This method produces directly onto a substrate well-defined polygon organic thin crystals with uniform thickness. The thin crystals are found to be single crystals of high quality. We show various illustrations including thiophene/phenylene co-oligomers and an oligophenylene. The organic crystal transistors based on these crystals showed good device performance. These thin single crystals are expected to be suitably applied to electronic devices.

## Introduction

Performance of organic devices strongly depends on molecular arrangement. Enhanced characteristics are expected along specified axial directions for the organic molecular crystals. Regular arrangement of the molecules is responsible for the improved carrier transport,[1−6] the polarized emission,[7−9] and the spectrally narrowed emission[10−13] in organic crystals comprising $\pi$-conjugated molecules. It will, therefore, be important to make the most use of organic crystals with highly aligned molecules in device configurations. In this context, recently, progress has been made in the device fabrication; examples include direct lamination of organic crystals on the device substrate.[2,4,5] The method might, however, be susceptible to, e.g., lamination conditions. Mas-Torrent et al. reported the fabrication of single crystals by drop-casting solution onto the device substrate.[6] The resulting crystals exhibited pretty high mobility up to 1.4 $cm^2$/Vs. This technique, however, is not applicable to the materials of poor solubility in the solvent. Practically, pentacene, which is assumed to be one of the best candidates for the organic field-effect transistors (OFETs), is sparingly soluble in organic solvents.[14] This has motivated us to develop a new method of bringing an organic crystal in sure contact with a substrate. In the present studies, we have developed a novel crystal-growth method that enables direct formation of organic thin single crystals on the substrate.

The method is characterized by direct film deposition onto the substrate in a liquid phase. The said substrate is connected to a thermal radiator (consisting of, e.g., a metal plate), allowing the substrate to be cooled locally in the liquid. This causes the organic material in the liquid phase to be effectively deposited onto the substrate through recrystallization. Thus, the material ends up as thin single crystals of high quality in firm contact with the substrate. Here, we exclusively used for the substrate a silicon wafer with oxidized silicon on its surface. The resulting thin single crystals grown on top of this substrate are characterized by the presence of the vertically aligned molecules against the substrate.[15] Organic materials can be hard to dissolve completely depending on their chemical species. The present method is effective even on such occasions, where we use a mixture of an organic powder material and a saturated solution. In the present studies, we show various examples of the crystal growth for organic semiconductors. These include thiophene/phenylene co-oligomers (TPCOs), a newly occurring class of molecular semiconductors, together with an oligophenylene. The thin single crystals grown on the silicon substrate can immediately serve for the device fabrication. We made the OFET devices with these thin crystals and examined the device performance.

* Corresponding author. E-mail: yamao@kit.ac.jp. Tel.: 81-75-724-7780. Fax: 81-75-724-7800.

† Current address: the Furukawa Electric Co., Ltd., 5-1-9 Higashi-Yawata, Hiratsuka 254-0016, Japan.

(1) Briseno, A. L.; Tseng, R. J.; Ling, M.-M.; Falcao, E. H. L.; Yang, Y.; Wudl, F.; Bao, Z. *Adv. Mater.* **2006**, *18*, 2320−2324.
(2) (a) Sundar, V. C.; Zaumseil, J.; Podzorov, V.; Menard, E.; Willett, R. L.; Someya, T.; Gershenson, M. E.; Rogers, J. A. *Science* **2004**, *303*, 1644−1646. (b) Menard, E.; Podzorov, V.; Hur, S.-H.; Gaur, A.; Gershenson, M. E.; Rogers, J. A. *Adv. Mater.* **2004**, *16*, 2097−2101. (c) Podzorov, V.; Menard, E.; Borissov, A.; Kiryukhin, V.; Rogers, J. A.; Gershenson, M. E. *Phys. Rev. Lett.* **2004**, *93*, 086602.
(3) Zeis, R.; Siegrist, T.; Kloc, Ch. *Appl. Phys. Lett.* **2005**, *86*, 022103.
(4) (a) Nakamura, K.; Ichikawa, M.; Fushiki, R.; Kamikawa, T.; Inoue, M.; Koyama, T.; Taniguchi, Y. *Jpn. J. Appl. Phys.* **2005**, *44*, L1367−L1369. (b) Nakamura, K.; Ichikawa, M.; Fushiki, R.; Kamikawa, T.; Inoue, M.; Koyama, T.; Taniguchi, Y. *Jpn. J. Appl. Phys.* **2004**, *43*, L100−L102.
(5) Ichikawa, M.; Yanagi, H.; Shimizu, Y.; Hotta, S.; Suganuma, N.; Koyama, T.; Taniguchi, Y. *Adv. Mater.* **2002**, *14*, 1272−1275.
(6) Mas-Torrent, M.; Durkut, M.; Hadley, P.; Ribas, X.; Rovira, C. *J. Am. Chem. Soc.* **2004**, *126*, 984−985.
(7) Yanagi, H.; Morikawa, T. *Appl. Phys. Lett.* **1999**, *75*, 187−189.
(8) Yamada, Y.; Yanagi, H. *Appl. Phys. Lett.* **2000**, *76*, 3406−3408.
(9) Yanagi, H.; Morikawa, T.; Hotta, S.; Yase, K. *Adv. Mater.* **2001**, *13*, 313−317.
(10) Nagawa, M.; Hibino, R.; Hotta, S.; Yanagi, H.; Ichikawa, M.; Koyama, T.; Taniguchi, Y. *Appl. Phys. Lett.* **2002**, *80*, 544−546.
(11) Ichikawa, M.; Hibino, R.; Inoue, M.; Haritani, T.; Hotta, S.; Koyama, T.; Taniguchi, Y. *Adv. Mater.* **2003**, *15*, 213−217.
(12) Shimizu, K.; Hoshino, D.; Hotta, S. *Appl. Phys. Lett.* **2003**, *83*, 4494−4496.
(13) Bando, K.; Nakamura, T.; Masumoto, Y.; Sasaki, F.; Kobayashi, S.; Hotta, S. *J. Appl. Phys.* **2006**, *99*, 013518.
(14) Minakata, T.; Natsume, Y. *Synth. Met.* **2005**, *153*, 1−4.
(15) Hotta, S.; Waragai, K. *Adv. Mater.* **1993**, *5*, 896−908.

10.1021/cm071051z CCC: $37.00 
Published on Web 06/30/2007

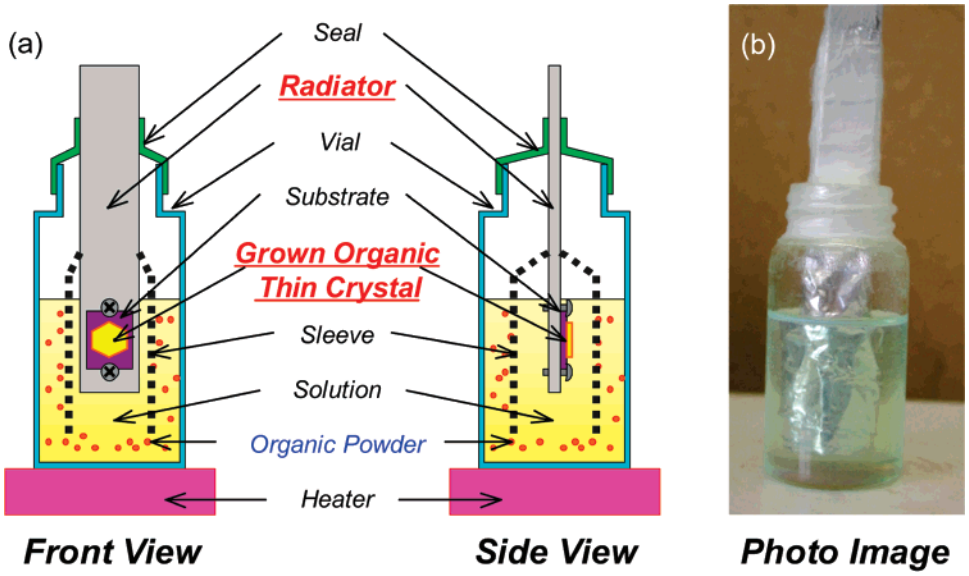


**Figure 1.** (a) Schematic diagram of the liquid-phase-growth apparatus; (b) photograph of the apparatus.

**Table 1. Used Solvent, Heater Temperature, and Growth Time for Each TPCO Material and Quaterphenyl**

| materials | solvents | heater temperature (°C) | growth time (h) |
|---|---|---|---|
| AC5 | monochlorobenzene | 60[a] | 86[a] |
| BP1T | monochlorobenzene | 80[a] | 72[a] |
| BP3T | 1-methylnaphthalene | 190[a] | 45[a] |
| BP4T | 1,2,4-trichlorobenzene | 100 | 48 |
| BP1T-OMe | 1,2,4-trichlorobenzene | 130[a] | 87[a] |
| BP1T-Bu | monochlorobenzene | 90 | 91 |
| BP2T-OMe | 1,2,4-trichlorobenzene | 190 | 48 |
| BP2T-He | 1,2,4-trichlorobenzene | 90 | 41.5 |
| AC5-$CF_3$ | monochlorobenzene | 80 | 73 |
| 4P | 1,2,4-trichlorobenzene | 80 | 74 |

[a] Typical value.

## Experimental Section

**Crystal-Growth Apparatus.** Figure 1 shows a schematic drawing of the crystal-growth apparatus in our studies as well as its picture. The mixture liquid is heated through the bottom of the vial. When the liquid is heated, the convection flow starts and the solution is transported toward the substrate. The substrate is wrapped with a sleeve of aluminum foil so that undissolved powder material is prevented from unintentionally attaching to the substrate. Although the presence of the undissolved powder material seems superfluous, that is not actually the case. It is because its presence is useful in automatically keeping the solution saturated and, hence, ensuring uniform deposition of the crystal. The solution is supplied with the solute from the powder material to maintain saturation immediately after portions of the solute in the solution are deposited as crystals onto the substrate. This also exonerates us from precisely controlling solution temperature or volatilization as in the conventional solution methods.

The growth apparatus is equipped with a radiator made of iron steel so that this radiator can release heat from the liquid to the atmosphere to cool the substrate locally and to keep its temperature lower than that of the surrounding liquid. This makes the crystals grow directly on the substrate. As an option, we can appropriately heat (or cool) the radiator and generate a suitable temperature difference between the radiator and the liquid to optimize the process of crystal growth. We also found it effective to use a shorter radiator. The "shorter radiator" means that the radiator outside the sealed glass apparatus is short, readily keeping its temperature inside the mixture relatively high. Preventing the radiator from being overcooled facilitates the growth of larger crystals.

**Materials Synthesis and Crystal Growth.** The TPCOs include AC5, BP1T, BP3T, BP4T, BP1T-OMe, BP1T-Bu, BP2T-OMe, BP2T-He, and AC5-$CF_3$. Structural formulas as well as abbreviated notations of the TPCOs are summarized in Figure 2. These TPCOs were synthesized and purified according to the literature methods.[16] Quaterphenyl (4P; Tokyo Kasei Kogyo, Co., Ltd.) was used as purchased without further purification. We used for solvent monochlorobenzene (in the case of making AC5, BP1T, BP1T-Bu, and AC5-$CF_3$ crystals), 1,2,4-trichlorobenzene (BP4T, BP1T-OMe, BP2T-OMe, BP2T-He, 4P), and 1-methylnaphthalene (BP3T). The solvents (monochlorobenzene and 1,2,4-trichlorobenzene from Kanto Chemical Co., Inc., and 1-methylnaphthalene from Sigma-Aldrich, Inc.) were used as purchased without further purification as well. Organic materials were crushed into powders in the solvent with an ultrasonic bath.

The mixture of the powders and solvent was sealed in a glass vial and heated by an electric heater. The thin crystals were grown on the quarried $SiO_2$/Si wafer that was chosen as the substrate and mounted on the iron steel radiator. Those thin crystals were obtained by heating the liquid at an appropriate temperature for an appropriate period of time depending on the chemical species of organic materials used for crystal growth. In the case of AC5, for instance, the liquid was heated and kept at 60 °C for 86 h. The TPCOs are less soluble with increasing molecular weights. In such cases, we used naphthalene derivatives as better solvents to make single crystals. The resulting crystals were cleansed by soaking them in acetone. Used solvents, heater temperatures, and growth times for all the materials are summarized in Table 1.

**Measurements.** The nonpolarizing and polarizing micrographs were taken through a NIKON ELIPSE LV100POL microscope with a Hg lamp. The X-ray diffractions were measured by a Rigaku RINT 2500 X-ray diffractometer with Cu Kα radiation. The thickness of the grown film was measured with an ULVAC DEKTAK-3ST surface profiler. The FETs were fabricated by depositing Au source and drain contacts on the grown crystals with a homemade vacuum evaporation equipment. The Au electrodes were deposited partly on the $SiO_2$ surface beyond the crystal. The evaporated Au contacts were further reinforced by successive Al deposition to secure steady electrical measurements. The back of

(16) (a) Hotta, S.; Kimura, H.; Lee, S. A.; Tamaki, T. *J. Heterocyclic Chem.* **2000**, *37*, 281−286. (b) Hotta, S.; Katagiri, T. *J. Heterocyclic Chem.* **2003**, *40*, 845−850. (c) Katagiri, T.; Ota, S.; Ohira, T.; Yamao, T.; Hotta, S. *J. Heterocyclic Chem.* **2007**, *44*, 853−862.

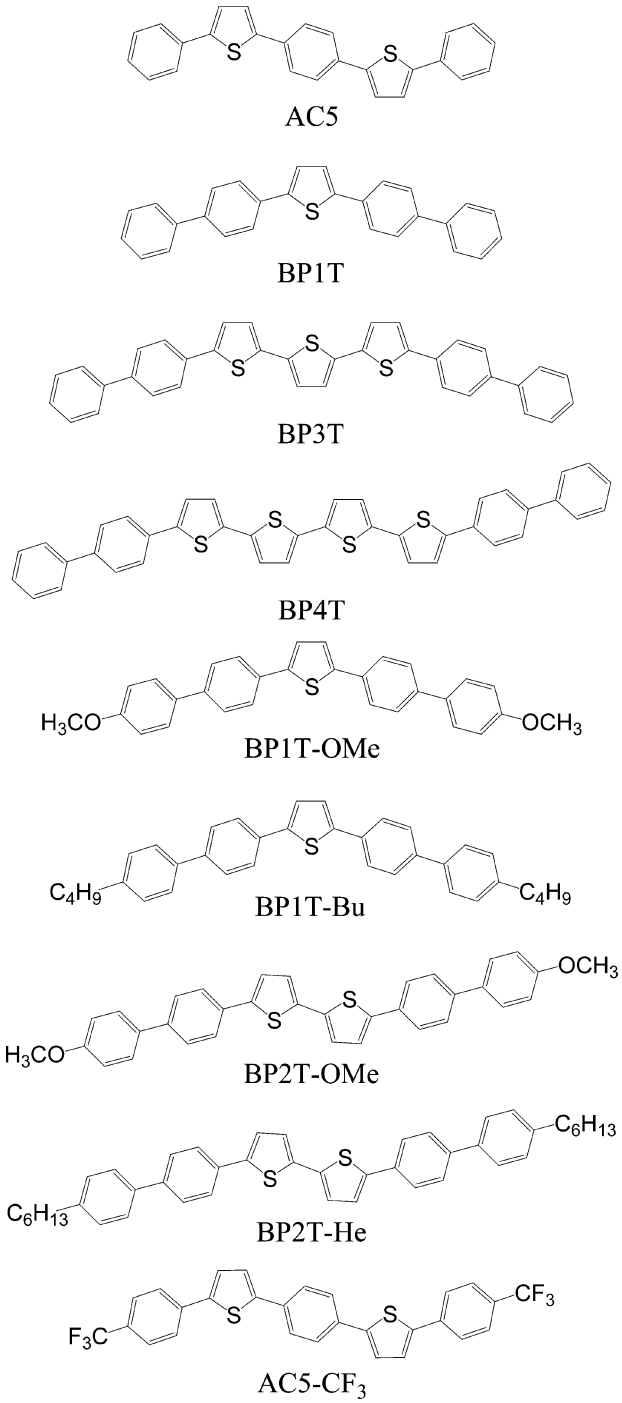


**Figure 2.** Structural formulas and abbreviated notations of the used thiophene/phenylene co-oligomers (TPCOs).

the $SiO_2$/Si wafer substrate was used as the gate contact, and the silicon dioxide layer was used for the gate insulator. The FET action characteristics were measured using an Agilent Technologies 4156B precision semiconductor parameter analyzer and an Advantest R6245 two-channel voltage current source/monitor under an ambient environment or under vacuum ($\sim 10^{-3}$ Pa).

## Results and Discussion

Nonpolarizing micrographs of an AC5 film are shown in parts a and b of Figure 3. Polarizing micrographs under the diagonal and extinction positions of the crossed nicol are shown in parts c and d of Figure 3, respectively. For comparison, a micrograph of AC5 powders (as a starting material) is shown in Figure 3e under the same magnification.

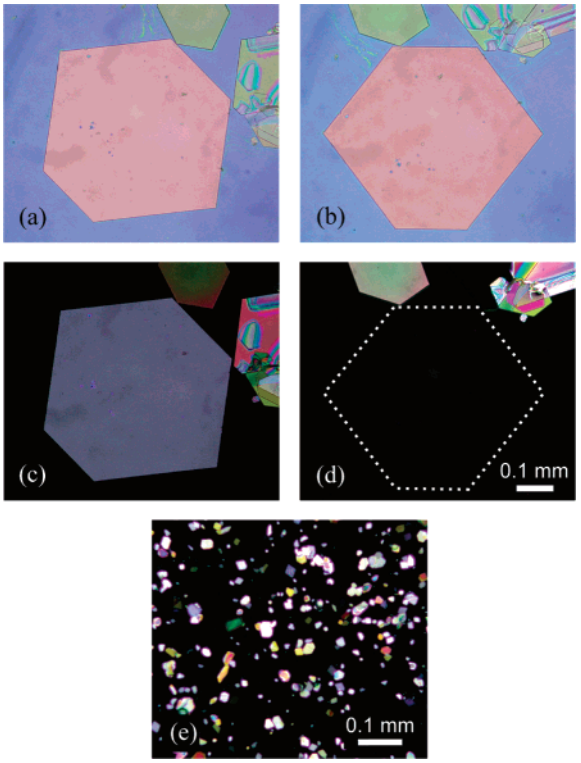


**Figure 3.** (a) and (b) Nonpolarizing micrographs of the AC5 thin crystal on a $SiO_2$/Si wafer substrate; (c) and (d) polarizing micrographs of the same AC5 thin crystal; (e) polarizing micrograph of AC5 powders (treated with an ultrasonic bath). The micrographs (c) and (d) were taken under the diagonal position and the extinction position (i.e., rotated by 45° relative to the diagonal position) of the crossed nicol, respectively. The nonpolarizing micrographs (a) and (b) correspond to (c) and (d) in view geometry, respectively.

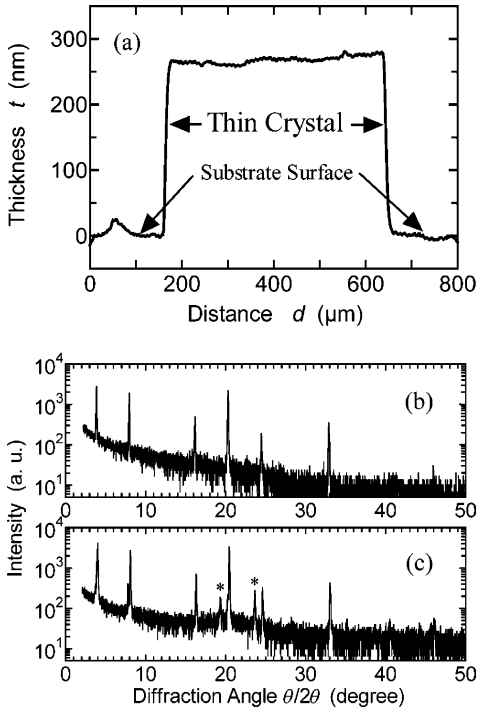


**Figure 4.** (a) Surface profile of the AC5 thin crystal. X-ray diffraction patterns of (b) the AC5 thin crystals on a $SiO_2$/Si wafer substrate and (c) the as-synthesized material of AC5 on a cover glass. The asterisks indicate the peaks that do not reflect the molecular length of AC5 (see text).

The microscope observations clearly indicate that each AC5 crystal film comprises a hexagon. The fact that the polarizing

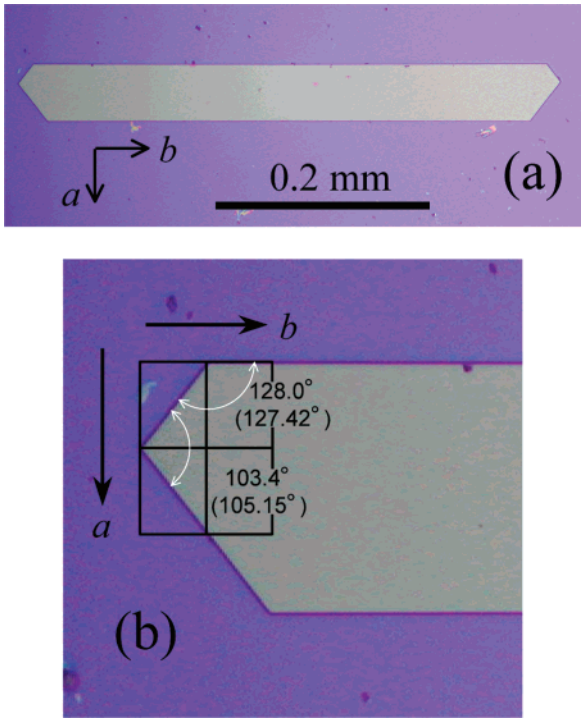


**Figure 5.** (a) Micrograph of the BP1T thin crystal on a $SiO_2$/Si wafer substrate; (b) enlarged micrograph of the crystal. The direction and relative magnitude of the *a*- and *b*-axes are indicated with the arrows and rectangles. The *b*-axis parallels the hexagon long sides. The specific angles (indicated with white arc arrows) read with a protractor are compared with those calculated from the crystallographic data[18a] that are given in parentheses.

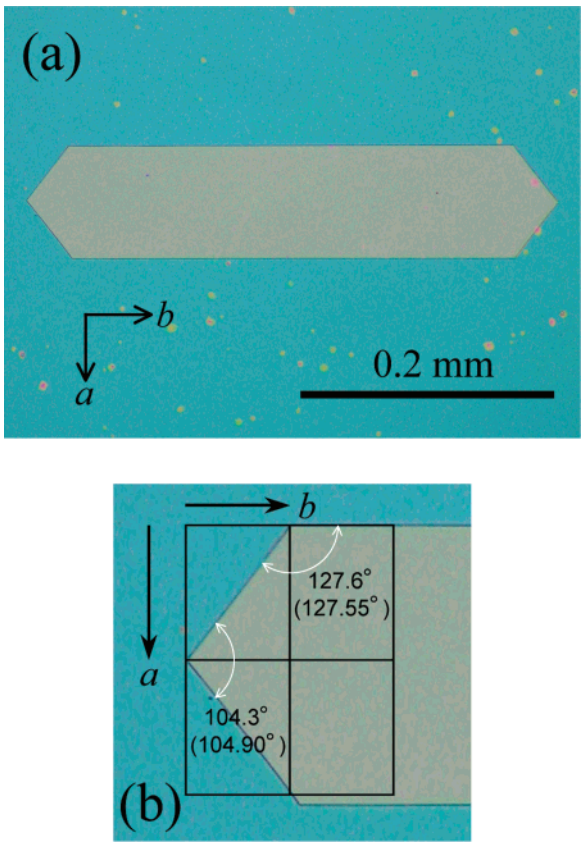


**Figure 6.** (a) Micrograph of the BP3T thin crystal on a $SiO_2$/Si wafer substrate; (b) enlarged micrograph of the crystal. The direction and relative magnitude of the *a*- and *b*-axes are indicated with the arrows and rectangles. The *b*-axis parallels the hexagon long sides. The specific angles (indicated with white arc arrows) read with a protractor are compared with those calculated from the crystallographic data[18b] that are given in parentheses.

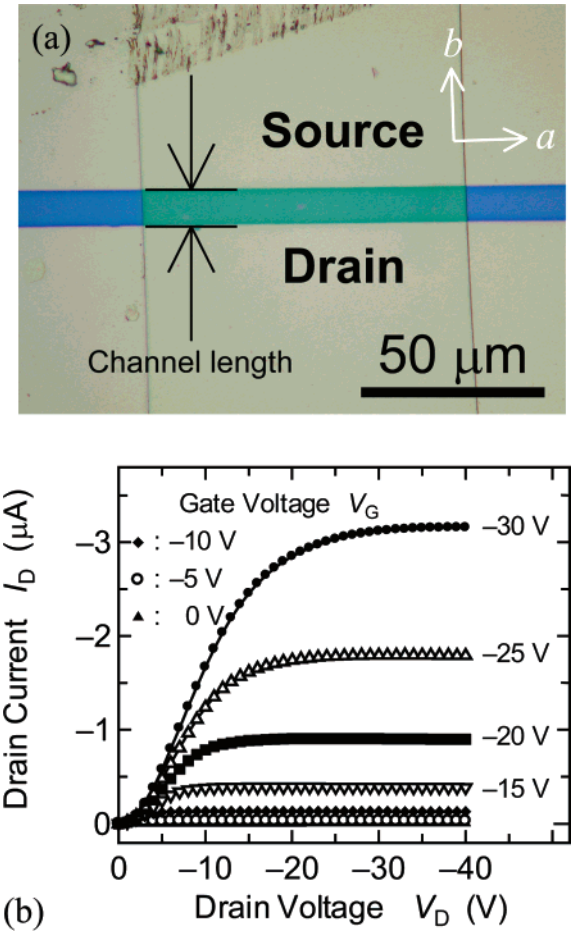


**Figure 7.** (a) Micrograph of the FET device made of a BP3T thin crystal. The channel of the device was formed along the crystal *b*-axis; (b) the characteristics of the BP3T FET device measured under an ambient environment.

micrograph of the AC5 film entirely vanishes at the extinction position [Figure 3d] demonstrates that the film is a single crystal.

To characterize the thin single crystals, we measured the thickness and X-ray diffraction of an AC5 crystal. The thickness of the crystal was estimated at approximately 270 nm and was uniform within the range of several nm (see Figure 4). The film thickness, however, differed from sample to sample. This probably reflects the difference in the growth time and/or rate of the individual crystals. Figure 4b shows the diffraction pattern for the AC5 thin single crystal as compared with that of the as-synthesized material (Figure 4c). In the thin single crystal, only the first- and higher-order peaks of the same diffracting plane are observed. The plane distance evaluated from diffraction peaks is $d = 21.65$ Å for Figure 4b, which reflects a molecular length of AC5.[17] This means that the single crystal consists of the regular molecular layered structure.[18] This structural characteristic is common to the thin crystals of other chemical species. As for the as-synthesized material, on the other hand, we noticed peaks occurring from planes other than that associated with the molecular length (denoted with asterisks in Figure 4c).

For BP1T and BP3T, we obtained long hexagon crystals and their typical sizes were ~0.5 mm in length and ~50−100 $\mu$m in width (Figures 5a and 6a, respectively). Since

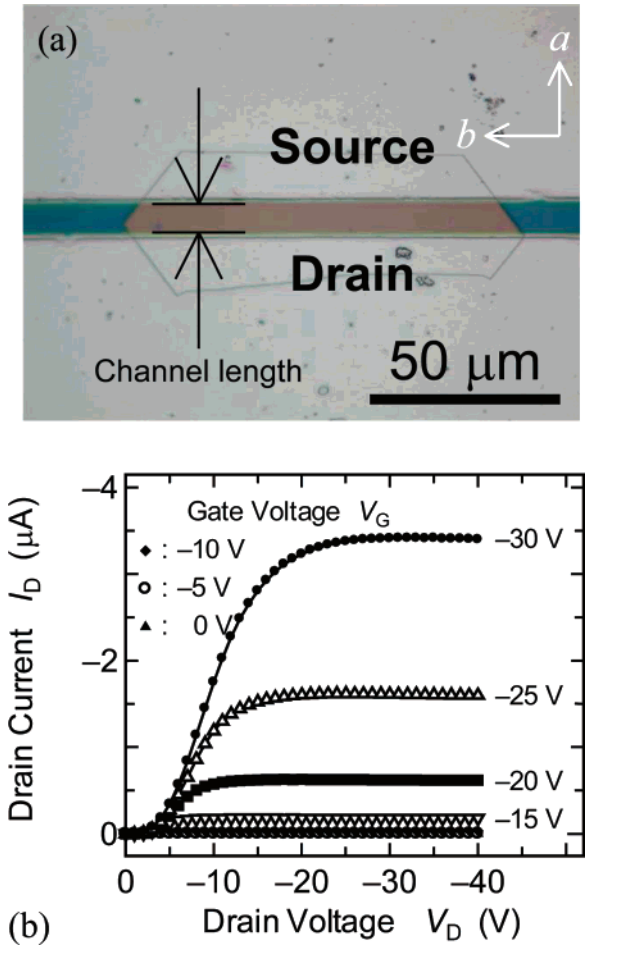


**Figure 8.** (a) Micrograph of the FET device made of another BP3T thin crystal. The channel of the device was formed along the crystal *a*-axis; (b) the characteristics of the BP3T FET device measured under an ambient environment.

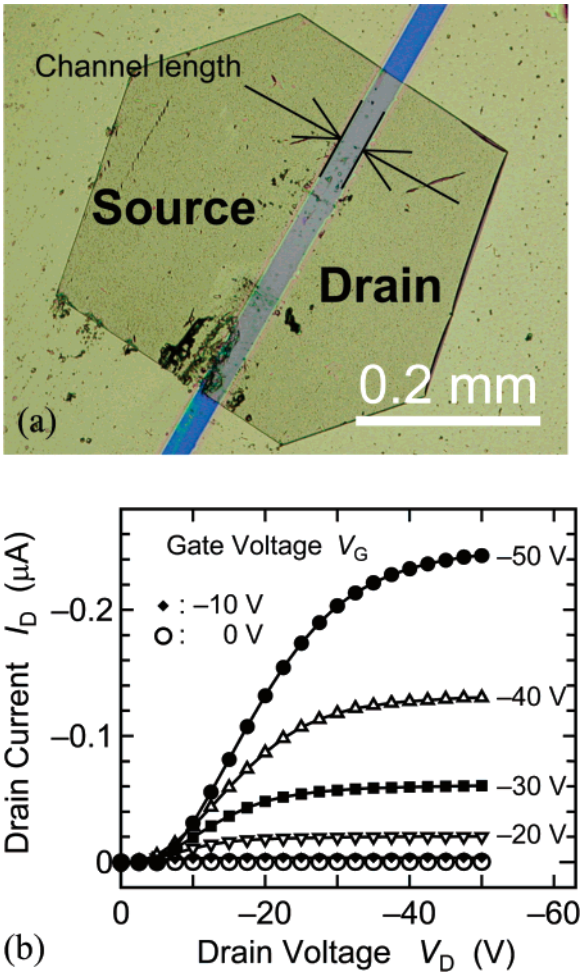


**Figure 9.** (a) Micrograph of the FET device made of an AC5 thin crystal; (b) the characteristics of the AC5 FET device measured under an ambient environment.

the crystal structures of these TPCO materials have successfully been determined by the X-ray analysis,[18] this allows us to assign the individual hexagon sides to the crystallographic axes or specific directions through the characteristic angles (i.e., the angles between the adjacent hexagon sides). Figures 5b and 6b indicate enlarged micrographs of each crystal. The direction and relative magnitude of the *a*- and *b*-axes are depicted in the figures. Both the angles read in the figures and those calculated from the crystallographic data[18] are in good agreement. With the BP3T crystal, for example, the read angle 104.3° (with a protractor) is almost the same as the calculated angle of 104.90°, as shown in Figure 6b. Thus, the geometrical characterization of the well-defined polygon crystals has fully been supported by the (polarizing) microscope observation and X-ray diffraction measurements.

It is worthy of note that, by conventional solution methods, it is difficult to create thin single crystals directly on substrates.[19,20] Here, we have a unique opportunity to explore the possibility of applying the present method to the device fabrication. To this end, we have fabricated field effect transistors (FETs) using the aforementioned thin single crystals. We made the top contact type devices. Photographs of the FET devices for BP3T thin crystals are shown in Figures 7a and 8a. The results of the electrical measurements show that the FETs are driven as p-type device (Figures 7b and 8b). Normal FET characteristics were observed. The determination of the crystallographic axes (i.e., the *a*- and *b*-axes) enables us to measure and define the mobility along those crystal axes. In Figures 7a and 8a, the source and drain contacts were made such that the channel were formed along the crystal *b*- and *a*-axes, respectively. The FET characteristics taken under an ambient environment were shown in Figures 7b and 8b. The calculated field effect mobilities along the *b*-axis (*a*-axis) were estimated at $8.7 \times 10^{-2}$ ($8.4 \times 10^{-2}$) and $1.3 \times 10^{-1}$ ($1.6 \times 10^{-1}$) cm$^2$/Vs at the linear and the saturation regions, respectively. These results are comparable to those by Yanagi et al.[21] The significant difference was not observed between the mobilities along the *a*- and *b*-axes.

(17) Hotta, S.; Ichino, Y.; Yoshida, Y.; Yoshida, M. *J. Phys. Chem. B* **2000**, *104*, 10316−10320.
(18) (a) Hotta, S.; Goto, M. *Adv. Mater.* **2002**, *14*, 498−501. (b) Hotta, S.; Goto, M.; Azumi, R.; Inoue, M.; Ichikawa, M.; Taniguchi, Y. *Chem. Mater.* **2004**, *16*, 237−241. (c) Hotta, S.; Goto, M.; Azumi, R. *Chem. Lett.* **2007**, *36*, 270−271.
(19) Batra, A. K.; Carmichael-Owens, C. R.; Simmons, M.; Aggarwal, M. D.; Lal, R. B. *Cryst. Res. Technol.* **2005**, *40*, 757−760.
(20) (a) Adachi, H.; Takahashi, Y.; Yabuzaki, J.; Mori, Y.; Sasaki, T. *J. Cryst. Growth* **1999**, *198/199*, 568−571. (b) Nagaoka, K.; Adachi, H.; Brahadeeswaran, S.; Higo, T.; Takagi, M.; Yoshimura, M.; Mori, Y.; Sasaki, T. *Jpn. J. Appl. Phys.* **2004**, *43*, L261−L263.
(21) Yanagi, H.; Araki, Y.; Ohara, T.; Hotta, S.; Ichikawa, M.; Taniguchi, Y. *Adv. Funct. Mater.* **2003**, *13*, 767−773.

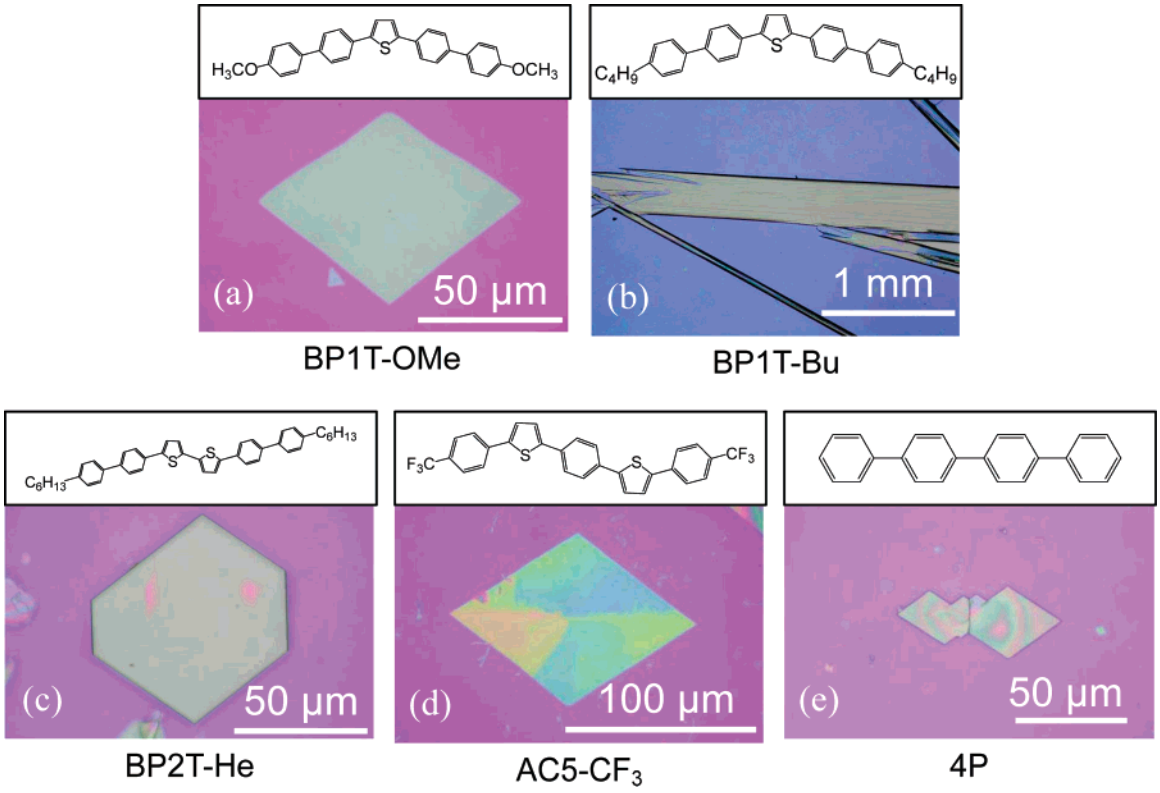


**Figure 10.** (a−e) Micrographs of thin crystals of several TPCO materials and quaterphenyl.

An upward curvature at low drain voltages noted in the device characteristic diagrams (Figures 7−9) was indicative of the presence of a contact resistance between the TPCO crystals and the source and drain electrodes. Further measurements with a device having a reduced contact resistance will be necessary for determining the anisotropic mobilities more precisely.

Similarly, we measured the mobilities of the FETs with various TPCOs either under an ambient environment or under vacuum. Again, we confirmed the normal FET characteristic. The mobilities of a thin single crystal of AC5 were $0.9 \times 10^{-3}$ and $1.7 \times 10^{-3}$ $cm^2/Vs$ (under an ambient environment) at the linear and the saturation regions, respectively (Figure 9). As further illustrations, the crystals of BP2T-OMe produced mobilities of $1.1 \times 10^{-2}$ $cm^2/Vs$ (under vacuum) at the linear region and $3.0 \times 10^{-2}$ $cm^2/Vs$ at the saturation region. The mobilities for BP4T were $3.0 \times 10^{-2}$ $cm^2/Vs$ and $7.7 \times 10^{-2}$ $cm^2/Vs$ (under vacuum) at the linear and the saturation regions, respectively. Thus, the thin single crystals of TPCOs produced well-defined FET characteristics. Regarding BP3T, we have been successful in measuring the mobilities along the crystallographic axes (the *a*- and *b*-axes), even though we were otherwise with the other materials.

Our new crystal-growth method can be applied to various organic materials. Several examples are depicted in parts a−e of Figure 10 with other TPCO materials with a variety of substituents on either molecular terminal[16c] and an oligophenylene. A variety of crystals with different sizes and shapes (e.g., hexagons, lozenges, swords, etc.) are readily available.

## Conclusion

We developed the novel and convenient method of crystal growth. Our improved method of crystal growth is characterized by using a glass apparatus equipped with an appropriately designed radiator. Organic semiconductors are dispersed in various solvents in the apparatus. This apparatus enables us to produce the organic thin single crystals of high quality. We have shown various illustrations including TPCOs and an oligophenylene. The well-defined polygon crystals are directly grown on a substrate with uniform thickness. The organic crystal transistors based on these crystals showed good device performance. These thin single crystals are expected to be suitably applied to electronic devices more generally.

**Acknowledgment.** This work was supported by a Grant-in-Aid for Science Research in a Priority Area "Super-Hierarchical Structures" (No. 17067009) from the Ministry of Education, Culture, Sports, Science and Technology, Japan.

CM071051Z